

Contribution from the Department of Chemistry—0506,
University of California, San Diego, La Jolla, California 92093-0506,
and Department of Chemistry, Indiana University, Bloomington, Indiana 47405

Ground-State Variability in μ_3 -Oxide Trinuclear Mixed-Valence Manganese Complexes: Spin Frustration

James K. McCusker,[†] Ho G. Jang,[†] Sheyi Wang,[§] George Christou,^{*§} and David N. Hendrickson^{*†}

Received January 15, 1992

A reexamination of bulk magnetic susceptibility data supplemented by variable-field magnetization and EPR studies definitively established the ground state of the mixed-valence complex $[\text{Mn}^{\text{II}}\text{Mn}^{\text{III}}\text{O}(\text{O}_2\text{CCH}_3)_6(\text{py})_3](\text{py})$ (**1**) as having $S = 3/2$, in contrast to the $S = 1/2$ ground state reported previously. This represents a rare example of a triangular μ_3 -oxide metal complex characterized as having an intermediate spin ground state (i.e., ground-state spin value other than the minimum available to the system). Variable-temperature susceptibility data measured at 10.00 kG were fit to a Heisenberg–Dirac–Van Vleck expression with $g = 2.05$, $J = -5.2 \text{ cm}^{-1}$, and $J^* = -2.7 \text{ cm}^{-1}$, where J characterizes the $\text{Mn}^{\text{II}}\text{--}\text{Mn}^{\text{III}}$ interaction and J^* the $\text{Mn}^{\text{II}}\text{--}\text{Mn}^{\text{II}}$ interaction. Variable-field magnetization data measured at 10.00, 30.00, and 48.00 kG in the range from 1.83 to 20.00 K were fit by full-matrix diagonalization to a spin Hamiltonian appropriate for a $S = 3/2$ state under the influence of axial zero-field splitting of the form $\hat{H} = D\hat{S}_z^2$. A fit was found for $g = 1.98$ and $D = 3.1 \text{ cm}^{-1}$. X-band EPR spectra measured from 2 to 30 K on a polycrystalline sample of **1** show several transitions in the $g \approx 2$ and $g \approx 4$ regions; the $g \approx 4$ signal decreases in intensity with increasing temperature, consistent with the assignment of a $S = 3/2$ ground state. Susceptibility data were also reanalyzed for the related mixed-valence complex $[\text{Mn}^{\text{II}}\text{Mn}^{\text{III}}\text{O}(\text{O}_2\text{CPh})_6(\text{py})_2(\text{H}_2\text{O})] \cdot 1/2(\text{CH}_3\text{CN})$ (**2**). On the basis of susceptibility data determined at 10.00 kG and X-band EPR spectra from 4 to 31 K, the ground state for complex **2** is assigned as $S = 1/2$. Fitting parameters for complex **2** were found to be $g = 1.99$, $J = -6.5 \text{ cm}^{-1}$, and $J^* = -4.5 \text{ cm}^{-1}$. The results for both complexes are discussed in terms of spin frustration within the Mn_3O core. In addition, the observation of multiple EPR-active states is discussed relative to the origin of EPR transitions from the oxygen-evolving complex of photosystem II.

Introduction

The electronic structure of trinuclear μ_3 -oxide transition metal complexes of the general formula $[\text{M}_3\text{O}(\text{O}_2\text{CR})_6\text{L}_3]^{n+}\text{S}$ has been the subject of extensive study over the past decade.¹ From studies of intermolecular energy transfer in Cr^{III} complexes² to the role of cocrystallized solvent S on intramolecular electron transfer in mixed-valence $\text{Fe}^{\text{II}}\text{Fe}^{\text{III}}$ systems,³ these complexes have provided an opportunity to examine critically theories of exchange interactions⁴ and electron transfer,⁵ in addition to allowing for detailed experimental and theoretical studies of the nature of cooperative interactions in the solid state.^{3,6} By far the most intensely studied of these μ_3 -oxide complexes are the iron-containing complexes. It has been found that in many cases a simple isotropic Heisenberg-type interaction of the form $\hat{H} = -2J_{ij}\hat{S}_i\hat{S}_j$ does not adequately describe the magnetic exchange interactions present in these iron complexes. A wide variety of theoretical models have been examined involving intercluster,⁷ biquadratic,⁸ and resonance exchange interactions⁹ to describe the electronic structures of these complexes.

Considerably less work has been directed toward the analogous manganese complexes, although both mixed-valence $\text{Mn}^{\text{II}}\text{Mn}^{\text{III}}$ and isovalent Mn_3^{III} complexes have been reported.¹⁰ Vincent et al.^{10a} reported the magnetochemistry of several μ_3 -oxide manganese complexes of the general formulation $[\text{Mn}_3\text{O}(\text{O}_2\text{CR})_6\text{L}_3]^{0,+}$, where R = Me or Ph and L is a neutral donor group such as pyridine or H_2O . Ground states with $S = 1/2$ were reported for the two mixed-valence $\text{Mn}^{\text{II}}\text{Mn}^{\text{III}}$ complexes. This is consistent with the literature where, with few exceptions,¹¹ the ground states of μ_3 -oxide complexes correspond to a minimum number of unpaired electrons (i.e., $S = 1/2$ for Fe^{III} and Mn^{II} , Mn^{III} ; $S = 0$ for $\text{Fe}^{\text{II}}\text{Fe}^{\text{III}}$ and Mn^{III} complexes). However, it is by no means obvious that the ground state of a $\text{Mn}^{\text{II}}\text{Mn}^{\text{III}}$ complex should have $S = 1/2$ since the total spin of such a complex can range from $S = 1/2$ to $S = 13/2$. In fact, the ground state in many of these complexes results from spin frustration.¹² This term describes an effect whereby the interplay of various exchange interactions in a polynuclear complex causes a net spin vector alignment which is different than that expected upon consideration of pairwise exchange interactions. By varying the ratio of exchange parameters in a M_3O complex, without making large

changes in J_{ij} parameters, it should be possible to stabilize ground states with $S \neq 1/2$ for a $\text{Mn}^{\text{II}}\text{Mn}^{\text{III}}$ complex.

- (1) For a recent review, see: Cannon, R. D.; White, R. P. *Prog. Inorg. Chem.* **1988**, *36*, 195.
- (2) (a) Dubicki, L.; Ferguson, J.; Williamson, B. *Inorg. Chem.* **1983**, *22*, 3220. (b) Schenk, K. J.; Gudel, H. U. *Inorg. Chem.* **1982**, *21*, 2253. (c) Wroblecki, J. T.; Dziobkowski, C. T.; Brown, D. B. *Inorg. Chem.* **1981**, *20*, 684.
- (3) (a) Jang, H. G.; Geib, S. J.; Kaneko, Y.; Nakano, M.; Sorai, M.; Rheingold, A. L.; Montrez, B.; Hendrickson, D. N. *J. Am. Chem. Soc.* **1989**, *111*, 173, and references therein. (b) Hendrickson, D. N.; Oh, S. M.; Dong, T.-Y.; Kambara, T.; Cohn, M. J.; Moore, M. F. *Comments Inorg. Chem.* **1985**, *4*, 329. (c) Hendrickson, D. N. Electron Transfer in Mixed-Valence Complexes in the Solid State. In *Mixed-Valency Systems: Applications in Chemistry, Physics, and Biology*; Prassides, K., Ed.; Kluwer Academic Publishers: Hingham, MA, 1991; pp 67–90.
- (4) For reviews on exchange interactions in transition metal systems, see: (a) Hatfield, W. E. Properties of Magnetically Condensed Compounds. In *Theory and Applications of Molecular Paramagnetism*; Boudreaux, E. A.; Mulay, L. N., Eds.; John Wiley and Sons, Inc.: New York, 1976. (b) Griffith, J. S. *Struct. Bonding (Berlin)* **1972**, *10*, 87. (c) O'Connor, C. J. *Prog. Inorg. Chem.* **1982**, *29*, 203. (d) Tsukerblat, B. S.; Belinskii, M. I.; Fainzil'berg, V. E. *Sov. Sci. Rev. B Chem.* **1987**, *9*, 337.
- (5) For reviews on electron transfer, see: (a) DeVault, D. *Quantum Mechanical Tunneling in Biological Systems*, 2nd ed.; Cambridge University Press: Cambridge, UK, 1984. (b) Cannon, R. D. *Electron Transfer Reactions*; Butterworths: Boston, 1980. (c) Mikkelsen, K. V.; Ratner, M. A. *Chem. Rev.* **1987**, *87*, 113.
- (6) (a) Sorai, M.; Hendrickson, D. N. *Pure Appl. Chem.* **1991**, *63*, 1503. (b) Stratt, R. M.; Adachi, S. H. *J. Chem. Phys.* **1987**, *86*, 7156. (c) Kambara, T.; Hendrickson, D. N.; Sorai, M.; Oh, S. M. *J. Chem. Phys.* **1987**, *85*, 2895.
- (7) (a) Dziobkowski, C. T.; Wroblecki, J. T.; Brown, D. B. *Inorg. Chem.* **1981**, *20*, 671. (b) Tsukerblat, B. S.; Belinskii, M. I.; Kuyavskaya, B. Ya. *Inorg. Chem.* **1983**, *22*, 995. (c) Gudel, H. U. *J. Chem. Phys.* **1985**, *82*, 2510.
- (8) (a) Uryu, N.; Friedburg, S. A. *Phys. Rev.* **1965**, *A140*, 183. (b) Rakitin, Y. V.; Zhemchuzhnikova, T. A.; Zelentsov, V. V. *Inorg. Chim. Acta* **1977**, *23*, 145.
- (9) For discussions on resonance exchange in general, see: (a) Papaefthymiou, V.; Girerd, J.-J.; Moura, I.; Moura, J. J. G.; Munck, E. *J. Am. Chem. Soc.* **1987**, *109*, 4703. (b) Noodleman, L.; Case, D. A.; Sontum, S. F. *J. Chem. Phys.* **1989**, *86*, 743, and references therein. For a detailed discussion of non-Heisenberg exchange, see ref 4d.
- (10) (a) Vincent, J. B.; Chang, H.-R.; Folting, K.; Huffman, J. C.; Christou, G.; Hendrickson, D. N. *J. Am. Chem. Soc.* **1987**, *109*, 5703. (b) Baikie, A. R. E.; Hursthouse, M. B.; New, D. B.; Thornton, P. J. *J. Chem. Soc., Chem. Commun.* **1978**, *62*. (c) Uemura, S.; Spencer, A.; Wilkinson, G. J. *J. Chem. Soc., Dalton Trans.* **1973**, 2565. (d) Baikie, A. R. E.; Hursthouse, M. B.; New, L.; Thornton, P.; White, R. G. *J. Chem. Soc., Chem. Commun.* **1980**, *64*. (e) Oh, S. M.; Hendrickson, D. N.; Hassett, K. L.; Davis, R. E. *J. Am. Chem. Soc.* **1985**, *107*, 8009. (f) Gomez-Garcia, C. J.; Coronado, E.; Pourroy, G. *J. Appl. Phys.* **1990**, *67*, 5992.

[†] University of California at San Diego.

[‡] Present address: Department of Chemistry, University of Minnesota.

[§] Indiana University.

This last point is of particular interest with respect to recent work by Kim et al.¹³ on the oxygen-evolving complex (OEC) of photosystem II (PSII) in green plant photosynthesis. The S_2 state of the OEC is believed to have a Mn_4 active site. Two EPR signals have been seen for the S_2 state. One signal has $g = 4.1$, and the other one is a multiline feature at $g = 2$. The relative intensities of these two signals depend on the sample history of the OEC. A substantial body of experimental data has been accumulated in the course of trying to assign the origins of the $g = 4.1$ and $g = 2$ transitions.¹⁴ Essentially two models have been proposed to account for these two S_2 -state EPR signals. Brudvig and co-workers¹⁵ proposed that both the $g = 4.1$ signal and the multiline $g \approx 2$ transition arise from different conformations of the same tetranuclear manganese complex. This model invokes a $S = 3/2$ ground state for the OEC and conformational changes in the protein which change the energy of an excited $S = 1/2$ state. In one conformation the $S = 1/2$ state is thermally accessible and EPR transitions from both the $S = 3/2$ ground state ($g = 4.1$) and the low-lying $S = 1/2$ excited state ($g \approx 2$) are observed. A change in the conformation of the protein presumably modifies the exchange interactions within the cluster, making the $S = 1/2$ excited state thermally inaccessible and leaving only the $g = 4.1$ signal of the $S = 3/2$ ground state. A second model has been put forth by Hansson et al.¹⁶ in which the $g = 4.1$ signal arises from a mononuclear Mn^{IV} site which exists in redox equilibrium with a binuclear exchange-coupled manganese site responsible for the $g \approx 2$ multiline pattern. The observation by Kim et al.¹³ of partially resolved manganese hyperfine lines for the $g = 4.1$ signal strongly indicates the $g = 4.1$ EPR signal is due to a multinuclear manganese site, in agreement with the model of Brudvig et al.¹⁵ Thus, it is important to discover what types of structural changes in a polynuclear mixed-valence manganese complex are required to change the distribution of low-energy spin states. It is also relevant to see if more than one state of such a complex can be EPR active.

Our recent work dealing with the effects of spin frustration in polynuclear transition metal complexes has shown that very subtle changes in the ratios of competing exchange interactions in a complex can have dramatic effects on the exact nature of ground and low-lying magnetic states.^{12,17} As a result of subtle changes in the exchange parameters characterizing the pairwise interactions in a complex, the spin of the ground state can change appreciably. In this paper we will show that for the mixed-valence complexes

$[Mn_3O(O_2CCH_3)_6(py)_3](py)$ (1) and $[Mn_3O(O_2CPh)_6(py)_2(H_2O)]^{1/2}(CH_3CN)$ (2) the former has a $S = 3/2$ ground state and the latter a $S = 1/2$ ground state. It is relevant to EPR work on the OEC site to note that both of these complexes exhibit EPR activity not only for the ground state but also for low-lying excited states.

Experimental Section

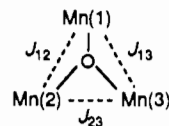
Syntheses. All compounds were prepared as previously described by Vincent et al.^{10a}

Magnetic Susceptibility Studies. Bulk susceptibility data measured at 10.00 kG were taken from Vincent et al.^{10a} and fit to the appropriate theoretical expression using a relative-error minimization routine.¹⁸ Variable-field magnetization data were measured for $[Mn_3O(O_2CCH_3)_6(py)_3](py)$ (1) as a function of temperature in applied fields of 10.00 (2.01–20.00 K), 30.00 (1.90–20.00 K), and 48.00 kG (1.83–15.00 K) using a Series 800 VTS-50 SQUID susceptometer (BTI, Inc., San Diego). A finely ground sample of complex 1 was immersed in a petroleum gel mull to prevent torquing of the crystallites at high magnetic fields. In none of the data was there any evidence of texturing due to anisotropy in the distribution of the sample relative to the applied field. The mass of the magnetization sample was calculated on the basis of the previously known susceptibility of the compound in an applied field of 10.00 kG for several temperatures above 5.00 K. Data were corrected for diamagnetism using Pascal's constants.¹⁹ All three isofield data sets were simultaneously fit to the appropriate spin Hamiltonian using a modified version of a previously reported full-matrix diagonalization program.²⁰

Electron Paramagnetic Resonance Spectroscopy. X-band EPR spectra for complex 1 and complex 2 were collected on a home-built spectrometer.²¹

Results and Discussion

Variable-Temperature 10-kG Susceptibility Data for $[Mn_3O(O_2CCH_3)_6(py)_3](py)$. The basic metal core of a triangular μ_3 -oxide complex can be represented schematically as



The spin Hamiltonian for this complex, assuming pairwise Heisenberg–Dirac–Van Vleck interactions is given in eq 1. For

$$\hat{H} = -2J_{12}\hat{S}_1 \cdot \hat{S}_2 - 2J_{13}\hat{S}_1 \cdot \hat{S}_3 - 2J_{23}\hat{S}_2 \cdot \hat{S}_3 \quad (1)$$

the two mixed-valence complexes being examined, it is reasonable to assume that the two $Mn^{II} \cdots Mn^{III}$ interactions are identical. If Mn(1) is assigned as the divalent ion, eq 1 reduces to eq 2, where

$$\hat{H} = -2J(\hat{S}_1 \cdot \hat{S}_2 + \hat{S}_1 \cdot \hat{S}_3) - 2J^* \hat{S}_2 \cdot \hat{S}_3 \quad (2)$$

$J = J_{12} = J_{13}$ and $J^* = J_{23}$. If a coupling scheme is defined with the total spin as $\hat{S}_T = \hat{S}_1 + \hat{S}_A$ and $\hat{S}_A = \hat{S}_2 + \hat{S}_3$ where \hat{S}_i is the spin operator for the i th metal center, the Kambe vector coupling approach²² can be used to generate an operator-equivalent expression for eq 2:

$$\hat{H} = -J(\hat{S}_T^2 - \hat{S}_A^2) - J^* \hat{S}_A^2 \quad (3)$$

Vincent et al.^{10a} used the eigenvalue expression which is readily obtained from eq 3 and obtained a fit of the 10-kG susceptibility data for $[Mn_3O(O_2CCH_3)_6(py)_3](py)$ (1); this fit is indicated in ref 10a. The best fit parameters were reported as $g = 2.13$, $J = -5.1 \text{ cm}^{-1}$, and $J^* = -8.3 \text{ cm}^{-1}$ with temperature-independent paramagnetism (TIP) fixed at 1×10^{-6} cgsu. These parameters

- (11) (a) One $Fe_3^{III}O$ complex has been reported to have a $S = 5/2$ ground state: Gorun, S. M.; Papaefthymiou, G. C.; Frankel, R. B.; Lippard, S. J. *J. Am. Chem. Soc.* **1987**, *109*, 4244. (b) A few $Fe^{II}Fe_2^{III}O$ complexes have been reported to have $S = 1$ ground states: see ref 1.
- (12) (a) McCusker, J. K.; Schmitt, E. A.; Hendrickson, D. N. High Spin Inorganic Clusters: Spin Frustration in Polynuclear Iron and Manganese Complexes. In *Magnetic Molecular Materials*; Gatteschi, D., Kahn, O., Miller, J. S., Palacio, F., Eds.; Kluwer Academic Publishers: Dordrecht, The Netherlands, 1991; pp 297–319. (b) McCusker, J. K.; Christmas, C. A.; Hagen, P. M.; Chadha, R. K.; Harvey, D. F.; Hendrickson, D. N. *J. Am. Chem. Soc.* **1991**, *113*, 6114. (c) Libby, E.; McCusker, J. K.; Schmitt, E. A.; Foltling, K.; Huffman, J. C.; Hendrickson, D. N.; Christou, G., *Inorg. Chem.* **1991**, *30*, 3486. (d) Harvey, D. F.; Christmas, C. A.; McCusker, J. K.; Hagen, P. M.; Chadha, R. K.; Hendrickson, D. N. *Angew. Chem., Int. Ed. Engl.* **1991**, *30*, 598.
- (13) Kim, D. H.; Britt, D.; Klein, M. P.; Sauer, K. *J. Am. Chem. Soc.* **1990**, *112*, 9389.
- (14) (a) Casey, J. L.; Sauer, K. *Biochim. Biophys. Acta* **1984**, *767*, 21. (b) Zimmermann, J. L.; Rutherford, A. W. *Biochim. Biophys. Acta* **1984**, *767*, 160. (c) Zimmermann, J. L.; Rutherford, A. W. *Biochemistry* **1986**, *25*, 4609. (d) Dismukes, G. C.; Siderer, Y. *Proc. Natl. Acad. Sci. U.S.A.* **1981**, *78*, 274. (e) de Paula, J. C.; Brudvig, G. W. *J. Am. Chem. Soc.* **1985**, *107*, 2643. (f) de Paula, J. C.; Beck, W. F.; Brudvig, G. W. *J. Am. Chem. Soc.* **1986**, *108*, 4002. (g) Beck, W. F.; Brudvig, G. W. *Biochemistry* **1986**, *25*, 6479.
- (15) (a) de Paula, J. C.; Beck, W. F.; Miller, A.-F.; Wilson, R. B.; Brudvig, G. W. *J. Chem. Soc., Faraday Trans. 1* **1987**, *83*, 3635. (b) de Paula, J. C.; Innes, J. B.; Brudvig, G. W. *Biochemistry* **1985**, *24*, 8114. (c) Brudvig, G. W. In *Advanced EPR, Applications in Biology and Biochemistry*; Hoff, A. J., Ed.; Elsevier: Amsterdam, 1989; p 839.
- (16) Hansson, O.; Aasa, R.; Vanngard, T. *Biophys. J.* **1987**, *51*, 825.
- (17) McCusker, J. K.; Vincent, J. B.; Schmitt, E. A.; Mino, M. L.; Shin, K.; Coggin, D. K.; Hagen, P. M.; Huffman, J. C.; Christou, G.; Hendrickson, D. N. *J. Am. Chem. Soc.* **1991**, *113*, 3012.

(18) Schmitt, E. A., unpublished results.

(19) *Theory and Applications of Molecular Paramagnetism*; Boudreaux, E. A., Mulay, L. N., Eds.; John Wiley and Sons: New York, 1976.

(20) Boyd, P. D. W.; Li, Q.; Vincent, J. B.; Foltling, K.; Chang, H.-R.; Streib, W. E.; Huffman, J. C.; Christou, G.; Hendrickson, D. N. *J. Am. Chem. Soc.* **1988**, *110*, 8537.

(21) Calvo, R.; Passeggi, M. C. G.; Isaacson, R. A.; Okamura, M. Y.; Feher, G. *Biophys. J.* **1990**, *58*, 149, and references therein.

(22) Kambe, K. *J. Phys. Soc. Jpn.* **1950**, *48*, 5.

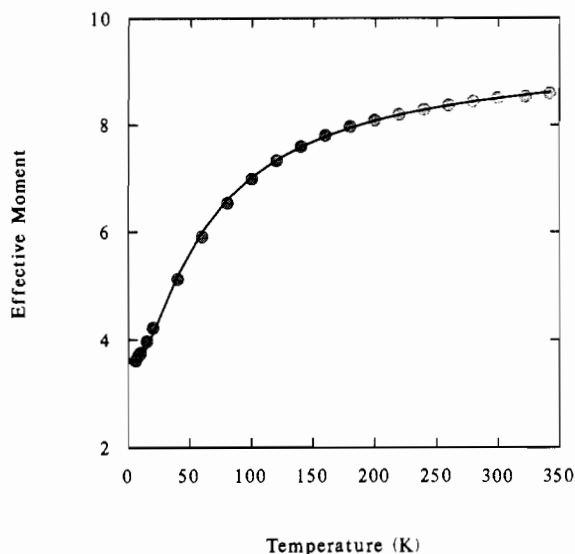


Figure 1. Plot of effective moment versus temperature for $[\text{Mn}_3\text{O}(\text{O}_2\text{CCH}_3)_6(\text{py})_3](\text{py})$ (1). Data were collected in an applied field of 10.00 kG. The solid line results from a fit of the data to the appropriate theoretical equation; see the text for parameters. The fit indicates a $S = 3/2$ ground state.

yield a $S = 1/2$ ground state ($S_A = 2$) with a $S = 3/2$ excited state ($S_A = 1$) approximately 2.5 cm^{-1} above the ground state. An additional $S = 3/2$ state ($S_A = 2$) is calculated to be approximately 15 cm^{-1} above the ground state.

An alternative description of the exchange interactions present in complex 1 was recently published by Gomez-Garcia et al.^{10f} In addition to HDVV exchange interactions, these authors suggest that, due to the mixed-valence nature of complex 1, a more accurate description of the electronic structure must include the effects of resonance exchange interactions. Gomez-Garcia et al. concluded that since the 223 K X-ray structure of complex 1 shows that the Mn_3O complex has C_3 symmetry, this complex is electronically delocalized. This means that there is no potential energy barrier for electron transfer. If this is the case, then resonance exchange should be included in the spin Hamiltonian. A spin Hamiltonian including resonance exchange (electron-transfer integral t) and HDVV exchange interactions with parameters J and J^* was employed. The 10-kG susceptibility data for complex 1 were fit by assuming D_{3h} symmetry; a fit of somewhat better quality than reported by Vincent et al. was found with parameters $J = -10.2 \text{ cm}^{-1}$, $J^* = -12.8 \text{ cm}^{-1}$, $g = 2.0$, and $t = 280 \text{ cm}^{-1}$. However, recent work²³ has shown that resonance exchange interactions are very likely not present in $[\text{Mn}_3\text{O}(\text{O}_2\text{CCH}_3)_6(\text{py})_3](\text{py})$. First, there is a first-order phase transition at 184.65 K observed in the heat capacity versus temperature data as determined by adiabatic calorimetry.^{23b} Below $\sim 185 \text{ K}$ the C_3 axis of the crystal is lost and each Mn_3O complex does not have C_3 symmetry. The results of a variable-temperature ^2H NMR study^{23a} for a single crystal of $[\text{Mn}_3\text{O}(\text{O}_2\text{CCD}_3)_6(\text{py})_3](\text{py})$ confirm that this complex is valence trapped below $\sim 185 \text{ K}$. IR data show that above $\sim 185 \text{ K}$ the complex is also trapped on the vibrational time scale. It is clear that above the 184.65 K abrupt phase transition this Mn_3O complex is rapidly interconverting between the four vibronic states on its ground-state potential energy surface. It does not become electronically delocalized in the 185–350 K range.

It was decided that the magnetic susceptibility characteristics of $[\text{Mn}_3\text{O}(\text{O}_2\text{CCH}_3)_6(\text{py})_3](\text{py})$ needed to be examined in more detail. A full examination of J , J^* parameter space gave an improved fit of the previously reported 10-kG data, shown in Figure 1. This fit was found with $g = 2.05$, $J = -5.2 \text{ cm}^{-1}$, and $J^* = -2.7 \text{ cm}^{-1}$; contributions from temperature-independent

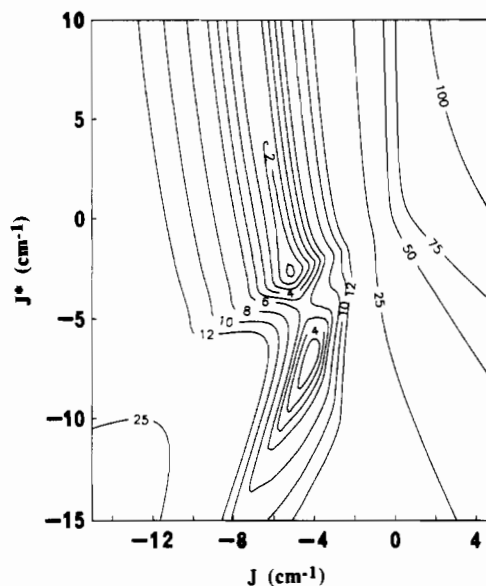


Figure 2. Relative error for fitting 10.00-kG susceptibility data of $[\text{Mn}_3\text{O}(\text{O}_2\text{CCH}_3)_6(\text{py})_3](\text{py})$ (1), calculated for $g = 2.05$. The figure is a two-dimensional projection of the surface, where the one local minimum and the global minimum can be seen.

paramagnetism and paramagnetic impurities were held fixed at 2.00×10^{-4} cgsu and 0.00%, respectively. It is clear that this latter set of parameters fits the susceptibility data for complex 1 somewhat better than those from Vincent et al. throughout the entire temperature range, except for a small deviation at the lowest temperatures (vide infra). The above parameters predict a $S = 3/2$ ground state ($S_A = 4$) for complex 1, in contrast to the $S = 1/2$ state ($S_A = 2$) based on the analysis by Vincent et al.^{10a} The important point to note is that although this new fit represents a nominally small change in the fitting parameters (primarily in the value of J^*), this small variation results in a change in the ground state of the molecule.

The plot in Figure 2 makes clear why Vincent et al.^{10a} found a fit where $J/J^* < 1$. In this figure is plotted an error contour map for fitting the susceptibility data of complex 1. It can be seen from this figure that the parameters corresponding to the fit by Vincent et al. represent a *local* minimum for these data, as opposed to the *global* minimum represented by the present analysis. The previous analysis of these data apparently fell into this sharply defined *local* minimum in the error surface potential. It was only by examining a wider range of parameter space and generating Figure 2 that we were able to identify the nature of this local minimum and find a better fit of the data.

Variable-Field Magnetization Studies. Low-temperature measurements of magnetization at variable magnetic field values provide a means to characterize the spin of the ground state. The presence of a large external field stabilizes one component (largest m_s value) of the ground state. If the temperature is low enough, all complexes will populate this lowest component and there is a saturation in the magnetization.

In Figure 3 are shown the results of variable-field magnetization studies carried out on complex 1 in applied fields of 10.00, 30.00, and 48.00 kG. At each field the temperature was varied (1.83–15.0 K at 48.00 kG, for example). The plot of reduced magnetization ($M/N\mu_B$, where N is Avogadro's number and μ_B is the Bohr magneton) as a function of H/T indicates at 48.00 kG a saturation of the magnetization of complex 1 at ~ 2.3 . This value is inconsistent with a $S = 1/2$ ground state and suggests a $S = 3/2$ ground state for the complex. The solid lines in the figure result from simultaneously fitting all three isofield data sets by means of a full-matrix diagonalization of a spin Hamiltonian appropriate for a $S = 3/2$ state under the influence of axial zero-field splitting of the form $H = D\hat{S}_z^2$. It should be pointed out that, owing to the small values of J and J^* , the energetic spacing of low-lying spin states is very small. In particular, $S =$

(23) (a) Jang, H. G.; Vincent, J. B.; Nakano, M.; Huffman, J. C.; Christou, G.; Sorai, M.; Wittebort, R. J.; Hendrickson, D. N. *J. Am. Chem. Soc.* **1989**, *111*, 7778. (b) Nakano, M.; Sorai, M.; Vincent, J. B.; Christou, G.; Jang, H. G.; Hendrickson, D. N. *Inorg. Chem.* **1989**, *28*, 4608.

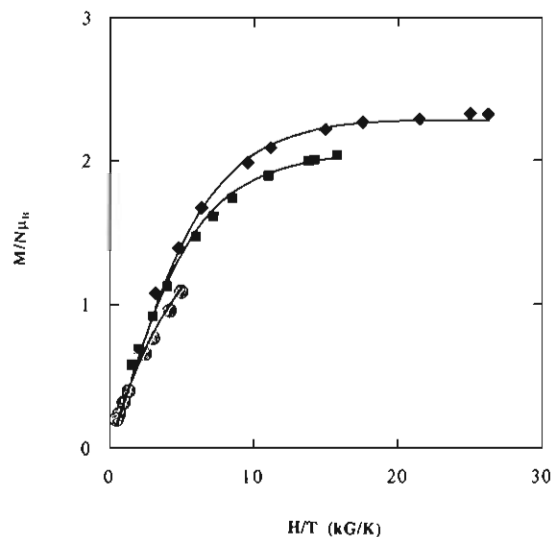


Figure 3. Plot of reduced magnetization versus magnetic field in units of temperature for $[\text{Mn}_3\text{O}(\text{O}_2\text{CCH}_3)_6(\text{py})_3](\text{py})$ (**1**) at (●) 10.00, (■) 30.00, and (◆) 48.00 kG. The three solid lines represent a fit to a spin Hamiltonian for a $S = 3/2$ state with axial zero-field splitting. See text for parameters.

$1/2$ and $S = 5/2$ states within 20 cm^{-1} of the ground state are likely populated at the highest temperatures of the magnetization data. However, since the saturation value of ~ 2.3 represents the lowest temperature of 1.83 K, we feel that treatment of the data in terms of an isolated ground state is a reasonable approximation. Thus it was assumed that only the $S = 3/2$ state is thermally populated and that the Zeeman interaction is isotropic. For each setting of the two parameters g and D , two 4×4 spin Hamiltonian matrices were diagonalized to get the eigenvalues; one matrix is for the parallel magnetic field and the other for the perpendicular orientation of the field. The magnetization was calculated as an average of the parallel and perpendicular components. An excellent fit was found for $g = 1.98$ and $D = 3.1 \text{ cm}^{-1}$. Attempts to fit these same data in terms of a $S = 1/2$ state resulted in g values in excess of 3, whereas a $S = 5/2$ ground-state description gave unacceptably low values for g (< 1.7). The value of D , although somewhat large, is not too surprising since both of the high-spin Mn^{III} ions are expected to contribute substantial zero-field effects due in part to the Jahn–Teller distortion in Mn^{III} complexes. The zero-field splitting found from the magnetization studies also explains the slight discrepancy between the experimental and calculated moments at low temperature for the fit of the bulk susceptibility data. The positive value for D indicates a net stabilization of the $m_s = \pm 1/2$ component of the $S = 3/2$ state, which will serve to depress the moment from that expected based solely upon an unsplit $S = 3/2$ state.

If the pairwise magnetic exchange interactions in complex **1** were negligibly small, then the spin-only value for a $\text{Mn}^{\text{II}}\text{Mn}^{\text{III}}_2$ complex would be expected to be $9.70 \mu_B$. At the highest temperature studied (342.0 K), the effective moment of complex **1** is $8.58 \mu_B$, or approximately 88% of the spin-only value. It is clear from the above fitting of the variable-temperature 10-kG data that the magnitudes of the exchange parameters in complex **1** are small. Thus, there are two possible explanations for the magnetization data in Figure 3. The ground state could have $S = 3/2$. On the other hand, it is possible that there is a $S = 1/2$ ground state with a very low-energy $S = 3/2$ excited state. As the magnetic field is increased from zero, the $M_s = -3/2$ component of this excited state could be stabilized enough to become the ground state at some value of magnetic field. The error surface in Figure 2 suggests that there is a $S = 3/2$ ground state. However, EPR experiments were carried out to decide between the two possibilities.

Electron Paramagnetic Resonance Spectroscopy. EPR spectroscopy has proven to be very useful in studying polynuclear manganese complexes which have half-integer spin states.²⁴ In

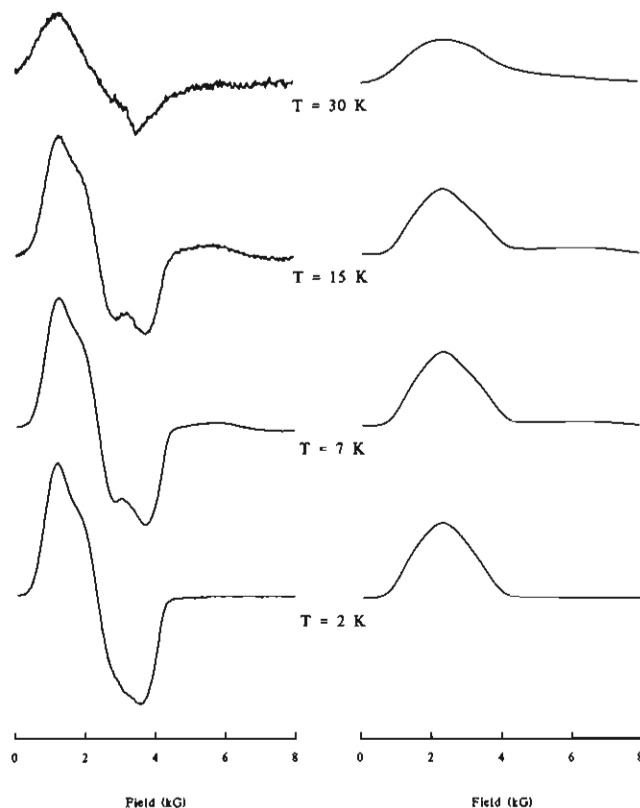


Figure 4. Temperature dependence of the X-band EPR spectrum of a polycrystalline sample of $[\text{Mn}_3\text{O}(\text{O}_2\text{CCH}_3)_6(\text{py})_3](\text{py})$ (**1**). The left-hand column shows the derivative plot, with the corresponding integration displayed in the right-hand column.

Figure 4 are shown the X-band EPR spectra for a polycrystalline sample of complex **1** in the range 2–30 K. These spectra show that the ground state of the complex **1** does, in fact, have $S = 3/2$ in accord with the fit in Figure 1. This conclusion is based on the fact that at 2 K there is a strong signal in the $g \approx 4$ region (actually split into two signals at 1250 G ($g = 5.0$) and ~ 2100 G ($g = 3.0$)). The intensity of this signal decreases with increasing temperature, indicating a depopulation of this state as the temperature is increased. This temperature dependence is consistent with the lowest energy state being the $\pm 1/2$ Kramers doublet from the $S = 3/2$ state. It is difficult from these spectra to determine how close in energy the $\pm 1/2$ ($S = 1/2$) and $\pm 3/2$ ($S = 3/2$) excited-state Kramers doublets are. However, the fit of the variable-field magnetization data for complex **1** is consistent with the $\pm 3/2$ Kramers doublet as being the lowest energy excited state. In fact, zero-field interactions could mix the $\pm 1/2$ ($S = 3/2$) and $\pm 1/2$ ($S = 1/2$) Kramers doublets.

In Figure 5 are plotted the eigenvalues from the variable-field magnetization analysis ($S = 3/2$ state only) in the field range examined in the EPR studies. In terms of assigning transitions observed in the 2 K spectrum, we can immediately ascribe a signal at $g \approx 2$ to the $m_s = -1/2 \rightarrow +1/2$ transition for H_{\parallel} . Likewise, there should be another transition at approximately 1600–1700 G from the lowest zero-field split component of the ground state for H_{\perp} . Based on the magnetization studies, these are the only two transitions which should be observed from the ground state, since the higher lying component of the $S = 3/2$ state is not split for H_{\perp} and the $m_s = -3/2 \rightarrow +3/2$ transition is forbidden for H_{\parallel} . However, as indicated above, it is clear that there are more than two transitions present in the spectrum. There are two possible origins for these additional absorptions: (a) the ground state,

(24) (a) Diril, H.; Chang, H.-R.; Nilges, M. J.; Zhang, X.; Potenza, J. A.; Schugar, H. J.; Isied, S. S.; Hendrickson, D. N. *J. Am. Chem. Soc.* **1989**, *111*, 5102, and references therein. (b) Dismukes, G. C. In *Mixed Valency Systems: Applications in Chemistry Physics and Biology*; Prassides, K., Ed.; Kluwer Academic Publishers: Hingham, MA, 1991; pp 137–154.

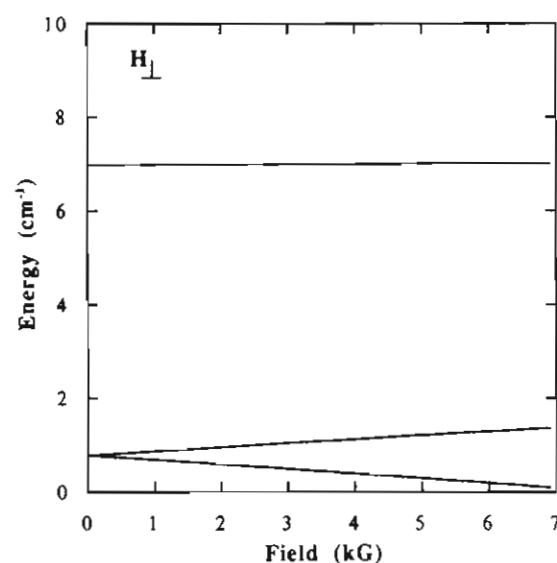
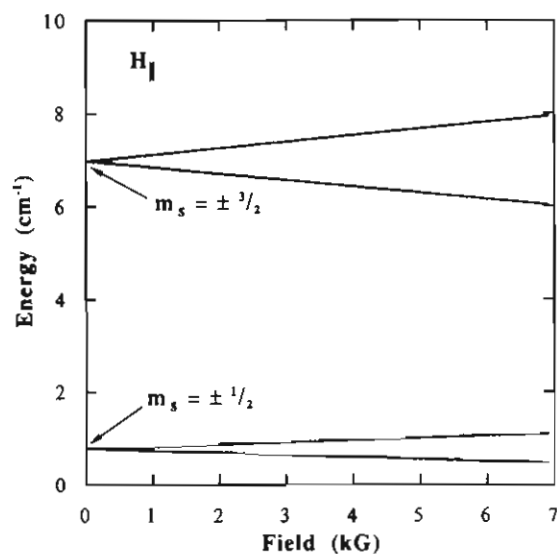


Figure 5. Eigenvalues from theoretical analysis of the magnetization data for $[\text{Mn}_3\text{O}(\text{O}_2\text{CCH}_3)_6(\text{py})_3](\text{py})$ (1). The field dependencies of the energies of the $\pm 1/2$ and $\pm 3/2$ Kramers doublets for the $S = 3/2$ ground state are shown. The direction of the applied field is indicated in the upper left corner of each plot.

although adequately handled by an axial term in the magnetization analysis, is actually split by a rhombic term; and (b) thermal population of excited states which are EPR active. The fact that the relative area of the $g \approx 2$ region increases with increasing temperature makes this latter option attractive in explaining the second transition in the $g \approx 2$ region.

In Figure 6 is plotted the Boltzmann distribution over the six lowest energy states based on the results of the magnetization studies and the bulk susceptibility measurements presented in Figure 1. The curve marked as 1 is obviously the population in the ground state, i.e., the lower energy $\pm 1/2$ Kramers doublet of the zero-field split $S = 3/2$ state. As discussed above, this Kramers doublet should give rise to two EPR transitions with $g_{\parallel} \approx 2$ and $g_{\perp} \approx 4$. Curve 2 gives the population in the $\pm 3/2$ Kramers doublet of the $S = 3/2$ state, which in the absence of rhombic zero-field splitting is EPR silent. Curve 3 is the population in the first excited spin state of the complex, which has $S = 1/2$. It is clear from this plot that this low-lying excited state, which would be expected to show a transition at $g \approx 2$, has some population at low temperature. Moreover, as the temperature is increased, the relative population of this state compared to the ground state increases. Curves 4–6 show the populations of higher lying excited states with $S = 1/2$, $S = 3/2$, and $S = 5/2$, respectively. None of these states are significantly populated at 2 K and therefore are not

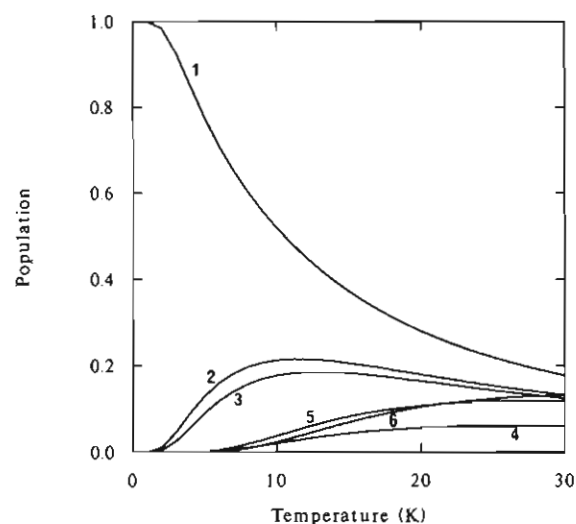


Figure 6. Calculated Boltzmann distributions for the six lowest energy states of $[\text{Mn}_3\text{O}(\text{O}_2\text{CCH}_3)_6(\text{py})_3](\text{py})$ (1). See text for details.

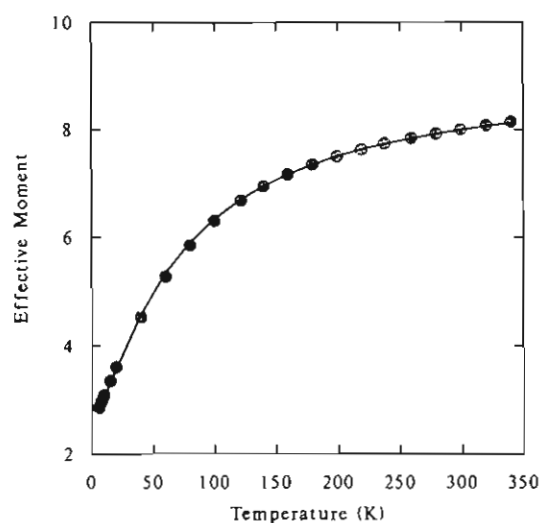


Figure 7. Plot of effective moment versus temperature for $[\text{Mn}_3\text{O}(\text{O}_2\text{CPh})_6(\text{py})_2(\text{H}_2\text{O})]^{1/2}(\text{CH}_3\text{CN})$ (2). Data were collected in an applied field of 10.00 kG. See text for parameters.

expected to contribute to the EPR spectrum at this temperature. Thus, we believe that the lowest lying $S = 1/2$ excited state is at least in part responsible for a second transition in the $g \approx 2$ region at 2 K and as well accounts for the increase in the area fraction observed between 2 and 15 K. Figure 6 reveals that all six states are significantly populated above 20 K, making specific interpretations of the spectrum collected at 30 K difficult.

Ground-State Variability: Effects of Ligand Substitution. On the basis of the above reexamination of the 10-kG susceptibility data for complex 1, we decided to take a second look at the data for the other mixed-valence manganese compound reported by Vincent and co-workers.^{10a} A plot of μ_{eff} versus temperature for $[\text{Mn}_3\text{O}(\text{O}_2\text{CPh})_6(\text{py})_2(\text{H}_2\text{O})]^{1/2}(\text{CH}_3\text{CN})$ (2) is given in Figure 7. The fitting by Vincent et al.^{10a} resulted in parameters of $g = 2.11$, $J = -7.3 \text{ cm}^{-1}$, and $J^* = -10.9 \text{ cm}^{-1}$. The solid line in Figure 7 is our refit of these data, which gave $g = 1.99$, $J = -6.5 \text{ cm}^{-1}$, and $J^* = -4.5 \text{ cm}^{-1}$ with the TIP and percent impurity fixed at 2.00×10^{-4} cgsu and 0.00%, respectively. Both analyses give $S = 1/2$ ground states, although the present fit gives a somewhat improved fit to the data for complex 2 than does that reported in ref 10a. The difference between the two fits lies predominantly in the ratio of J/J^* , where $J/J^* < 1$ for Vincent et al. and $J/J^* > 1$ for our analysis. In Figure 8 is shown a plot of the eigenstates of eq 3 as a function of this ratio calculated for $J < 0$ and $J^* < 0$ (i.e., both interactions are antiferromagnetic). It can be seen that although the nominal value of S_T is the same from both analyses, their positions on this plot and hence their excited spin

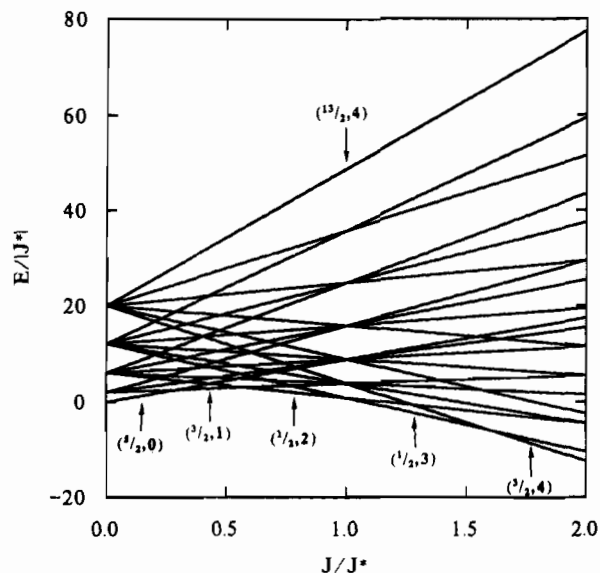


Figure 8. Plot of the eigenvalues of eq 3 calculated for $J < 0$ and $J^* < 0$ in units of $|J^*|$. States are labeled as (S_T, S_A) , where S_T is the total spin and S_A is the value from coupling of the spins of the two Mn^{III} ions.

state distributions are quite different. This is due to differences in the value of the S_A component comprising the ground state, where $S_A = 2$ from Vincent et al.^{10a} and $S_A = 3$ for the present fit. As with complex 1, an analysis of the relative error surface for fitting the susceptibility data of complex 2 reveals that the previous fit represents a local minimum, whereas the present fit represents the global minimum in parameter space.

X-band EPR spectra for a polycrystalline sample of complex 2 were collected in the range of 4–31 K and are given in Figure 9. These spectra clearly show that there is a change in the ground state of complex 2 relative to complex 1. The parameters found for complex 2 indicate the presence of a $S = 3/2$ state 3.8 cm^{-1} above the ground state. The EPR spectrum run at 4 K should thus be dominated by a signal from the $\pm 1/2$ ($S = 1/2$) Kramers doublet ground state. There could be a very small contribution from the low-lying $S = 3/2$ excited state. This is, in fact, what is observed for complex 2. At 4 K a broad signal ($\Delta H \approx 800 \text{ G}$) is observed at $g \approx 1.78$ with a weak signal at low field ($g \approx 4$). As the temperature is increased, the low-field signals increase in relative intensity. In the 31 K spectrum the bump at low field occurs at $g = 5.46$ (1180 G). This temperature dependence is roughly opposite to that observed in complex 1, consistent with predictions from Figure 8 which would indicate a reversal in the ordering of the lowest energy spin states between the two complexes. Furthermore, upon examination of the low-temperature μ_{eff} data for complex 2, it becomes clear that the ground and low-lying excited states of the two compounds must be different. The effective moment for complex 1 at 6.00 K is $3.61 \mu_B$ whereas for complex 2 it is $2.86 \mu_B$. While the data for complex 1 appear to exhibit a plateau, i.e., show a decrease in $\partial\mu_{\text{eff}}/\partial T$ below 10 K, a similar trend is not apparent in the data for complex 2. Thus, there is evidence even in the variable-temperature 10-kG susceptibility data that these two complexes have different ground states. This is confirmed by the EPR spectra.

The change in the ground state from $\pm 1/2$ ($S = 1/2$) Kramers doublet for complex 2 relative to the $\pm 1/2$ ($S = 3/2$) Kramers doublet ground state for complex 1 raises several issues which should be noted. The most important point is the fact that, upon substitution of H_2O for pyridine ligation on the Mn^{II} ion, the spin of the ground state has changed from $S = 3/2$ to $S = 1/2$. A comparison of the fitting parameters for the two complexes shows that this change results from only very minor changes in the absolute magnitudes of the exchange parameters. This serves to reiterate a point which we have made previously with regard to spin frustration in polynuclear transition metal complexes.^{12,17} This is the fact that very often it can be the ratio of competing coupling pathways and not so much their absolute magnitudes which

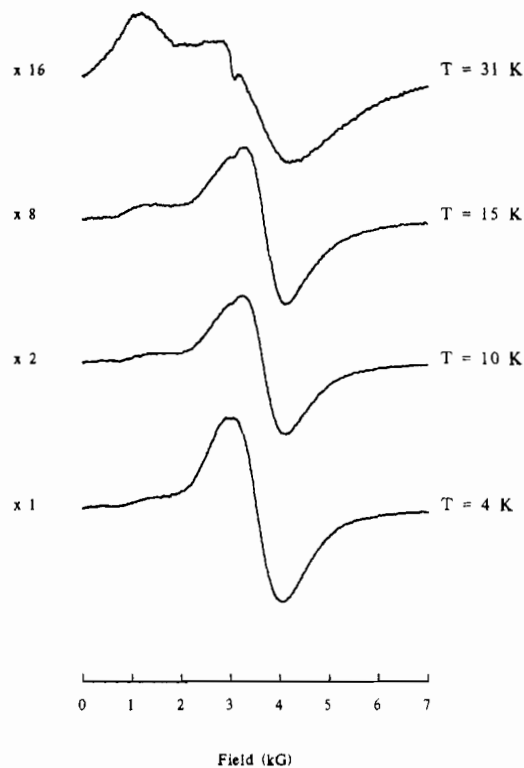


Figure 9. X-band EPR spectra for a powdered sample of $[Mn_3O(O_2CPh)_6(py)_2(H_2O)] \cdot \frac{1}{2}(CH_3CN)$ (2). Numbers in the left-hand column indicate relative spectrometer gain values.

characterizes the electronic structure of these complexes. Spin frustration is a concept which is readily understood in the context of triangular spin systems such as the μ_3 -oxide complexes considered here. The essence of the problem can be described as follows: if in the generalized Mn_3O triangular complex shown above all $Mn \cdots Mn$ interactions are antiferromagnetic and of the same magnitude and the spins on $Mn(1)$ and $Mn(2)$ align antiparallel, what orientation should the spin vector on $Mn(3)$ assume? In the case of complexes 1 and 2 where the mixed-valence nature of the system destroys the symmetry of the above problem, one needs to begin considering varying degrees of spin frustration. Thus, movement along the x -axis in Figure 8 can be likened to varying the degree of frustration, i.e., the dominance of one interaction over another within the molecule. The change in the ground state on going from complex 1 to complex 2 results from a decrease in the dominance of the J interaction over the J^* interaction. This decrease comes about even though the absolute magnitudes of the interactions are larger in the case of complex 2.

In terms of the nature of the two ground states, the $S = 3/2$ ground state in complex 1 is characterized by $S_A = 4$, whereas $S_A = 3$ for the $S = 1/2$ ground state in complex 2. Thus, as the ratio J/J^* decreases, the tendency to produce an antiparallel alignment of spins for the $Mn^{II} \cdots Mn^{III}$ interaction in complex 1 is countered somewhat in complex 2 due to the larger influence of the $Mn^{III} \cdots Mn^{III}$ interaction J^* . This gives a smaller value of S_A for complex 2 and a reduction in the total spin of the ground state. Note that if the situation were different, that is, if initially $J/J^* < 1$ and the system continued to favor J^* upon ligand substitution, the total spin of the system would have increased. It is not simply the fact that the magnitude of the coupling constants has increased slightly from complex 1 to complex 2 that caused the reduction in the spin of the ground state, but rather changes in the ratio J/J^* which dictated the trend. If, for example, the value of J increased to -10 cm^{-1} and J^* increased to -100 cm^{-1} , the ground state would have $S = 5/2$.

Concluding Comments

The reason for the observed changes in the coupling constants in complexes 1 and 2 is not clear. The changes are only on the

order of 1–2 cm⁻¹, vanishingly small compared to changes in bond energies and vibrational quanta which likely ensue following ligand substitution. It is likely that the changes reflect changes in the orbital energies on the Mn^{II} ion on going from a π acceptor ligand like pyridine in complex 1 to the relatively hard Lewis base H₂O in complex 2. This change likely has an effect on the energetics of through-bond interactions but trying to associate energy changes of a few wavenumbers to these geometric changes would be tenuous at best. In actuality, we feel that the difficulty in accounting for such a small change in energy is one of the attractive features of our results. That is, we have observed that very minor changes in the energies of pairwise exchange interactions can lead to a change in the ground state of a complex.

The present results do lend some support to the assertions by Brudvig et al.¹⁵ regarding the origins of the $g = 4.1$ and multiline $g \approx 2$ pattern from the OEC. Their model assigns both transitions as originating from the same tetranuclear complex, with changes in the conformation of the protein stabilizing or destabilizing a $S = 1/2$ excited state relative to the $S = 3/2$ ground state. We have shown it is possible to stabilize a $S = 3/2$ ground state in

a polynuclear Mn complex. Clearly, the oxidation states in complexes 1 and 2 bear little relation to what is likely present in S₂, but complex 1 is to our knowledge the first polynuclear Mn complex which has a well-characterized $S = 3/2$ ground state. Perhaps more importantly with respect to PSII is that there are strong indications from this work that by making relatively minor changes in the periphery of an exchange-coupled complex it is possible to significantly alter the electronic structure of a complex even to the extent of changing the ground state.

Acknowledgment. We thank Roger Isaacson of Professor George Feher's group (University of California at San Diego) for assistance in the collection of the EPR data. This work was supported by National Institutes of Health Grants HL13652 (D.N.H.) and GM39003 (G.C.).

Supplementary Material Available: Tables of magnetic susceptibility data and variable-field magnetization data for [Mn₃O(O₂CCH₃)₆(py)₃](1) and magnetic susceptibility data for [Mn₃O(O₂CPh)₆(py)₂(H₂O)]^{1/2}·CH₃CN (2) (3 pages). Ordering information is given on any current masthead page.

Contribution from the Department of Chemistry, Faculty of Science, The Australian National University, Canberra, ACT 2601, Australia

Dinuclear Complexes of Platinum with the 4,4'-Dipyrazolylmethane Ligand. Synthesis, Characterization, and X-ray Crystal Structure of γ -Bis(4,4'-dipyrazolylmethane-*N,N'*)bis[dichloroplatinum(II)]-*N,N*-Dimethylformamide (1/2) and Related Complexes

John A. Broomhead,* Louis M. Rendina,[†] and Meta Sterns

Received July 24, 1991

The preparation and characterization of novel platinum complexes with the 4,4'-dipyrazolylmethane (dpzm) ligand is described. Some proposed conformational isomers of the square-planar, dinuclear platinum(II) complexes α -[Cl₂Pt(μ -dpzm)₂PtCl₂]-0.5dmf, β -[Cl₂Pt(μ -dpzm)₂PtCl₂], and γ -[Cl₂Pt(dpzm)₂PtCl₂]-2dmf and the corresponding octahedral platinum(IV) complexes α -[Cl₄Pt(μ -dpzm)₂PtCl₄]-0.5H₂O and β -[Cl₄Pt(μ -dpzm)₂PtCl₄]-0.5dmf·0.5H₂O have been synthesized and characterized. Interconversion of the conformational forms for each oxidation state can be accomplished by various means. The mononuclear complexes *cis*-[PtCl₂(dmf)(dpzmH)]Cl and *cis*-[PtCl₄(dmf)(dpzmH)]Cl·0.5dmf and dinuclear mixed-oxidation state complex [Cl₄Pt(μ -dpzm)₂PtCl₂] were also prepared and characterized. The X-ray crystal structure determination of γ -[Cl₂Pt(dpzm)₂PtCl₂]-2dmf is reported. The complex exists as discrete molecular units with strong hydrogen-bonding to dmf solvent molecules. Each platinum atom is coordinated to two bridging dpzm ligands in a *cis* geometry. The crystals are monoclinic, space group *P*2₁/*n*, with cell parameters $a = 9.790$ (1) Å, $b = 13.444$ (2) Å, $c = 12.174$ (2) Å, $\beta = 105.74$ (1)°, and $Z = 2$. The structure was solved by the heavy-atom method and refined to $R = 0.036$ based on 2816 reflections.

Introduction

Apart from the work of Cuadro and others,¹ there have been no reports of complexes containing the 4,4'-dipyrazolylmethane (dpzm) ligand nor any studies of potential anticancer properties of its metal complexes. It is known that the ligand itself is not cytotoxic against HeLa cells *in vitro*.²

Dinuclear platinum(II) complexes have been described recently in a series of papers by Farrell et al.³⁻⁷ These show very good anticancer activity including activity toward cisplatin-resistant cell lines. The complexes possess two platinum centers which are bridged by a single diamine ligand such as 1,4-butanediamine. In contrast, the present work describes two platinum centers linked by two bridging ligands. Both types of dinuclear complexes represent new classes of anticancer agents. Unlike the aliphatic diamines used by Farrell and co-workers, the dpzm ligand is forced to act as a bridging bidentate ligand, being unable to form a chelate ring involving the same metal center. Some new mononuclear complexes of platinum(II) and -(IV) have also been isolated from acid solutions employing conditions similar to those

used by other workers.⁸ The *in vivo* anticancer drug screening and unique *in vitro* DNA-binding results for a selected number of complexes will be reported subsequently.⁹

Experimental Section

Materials and Methods. Elemental analyses were performed by the Australian National University Microanalytical Service. Platinum was determined gravimetrically following decomposition of the complex in N₂/methanol vapor. Pyrazole, methylene bromide, and methyl iodide were obtained commercially (Aldrich). The ligand dpzm was prepared

- (1) Cuadro, A. M.; Elguero, J.; Navarro, P.; Royer, E.; Santos, A. *Inorg. Chim. Acta* **1984**, *81*, 99.
- (2) Cuadro, A. M.; Elguero, J.; Navarro, P. *Chem. Pharm. Bull.* **1985**, *33*, 2535.
- (3) Farrell, N. P.; de Almeida, S. G.; Skov, K. A. *J. Am. Chem. Soc.* **1988**, *110*, 5018.
- (4) Roberts, J. D.; Van Houten, B.; Qu, Y.; Farrell, N. P. *Nucl. Acids Res.* **1989**, *17*, 9719.
- (5) Farrell, N.; Qu, Y.; Hacker, M. P. *J. Med. Chem.* **1990**, *33*, 2179.
- (6) Farrell, N.; Qu, Y.; Feng, L.; Van Houten, B. *Biochemistry* **1990**, *29*, 9522.
- (7) Qu, Y.; Farrell, N. *J. Inorg. Biochem.* **1990**, *40*, 255.
- (8) Van Kralingen, C. G.; de Ridder, J. K.; Reedijk, J. *Transition Met. Chem.* **1980**, *5*, 73.
- (9) Broomhead, J. A.; Rendina, L. M.; Webster, L. K. Manuscript in preparation.

[†] Present address: Research School of Chemistry, The Australian National University, Canberra, ACT 2601, Australia.